CONF-8809221--6

DEC 13 1989

SOME RECENT OBSERVATIONS ON THE RADIATION BEHAVIOR OF URANIUM SILICIDE DISPERSION FUEL*

CONF-8809221--6

DE90 003806

by

Gerard L. Hofman
Argonne National Laboratory
Argonne, Illinois 60439

To be Presented
at the

International Meeting on
Reduced Enrichment for Research and Test Reactors

September 19-22, 1988
San Diego, California

*Work supported by the U.S. Department of Energy under Contract No. W-31-109-ENG-38

Some Recent Observations on the Radiation Behavior of Uranium Silicide Dispersion Fuel

by

Gerard L. Hofman

Abstract

Addition of B_4C burnable poison results in higher plate swelling in both U_3Si_2 and U_3Si-Al dispersion fuel plates and also decreases the blister threshold temperature of these plates. Prolonged annealing of U_3Si_2-Al fuel plates produced no blister after 696 hours at 400°C. Blister formation started between 257 hours and 327 hours at 425°C and between 115 hours and 210 hours at 450°C.

Operation with breached cladding resulted in pillowing of an U_3Si-Al fuel plate due to reaction of the fuel core with coolant water.

I. Introduction

The miniplate irradiation program carried out in the Oak Ridge Research Reactor (ORR) has come to an end. Postirradiation analysis of the last batch of miniplates, as well as re-evaluation of previously reported results is in progress and will be reported in the next RERTR meeting.

This paper deals with some selected recent observations, the timely reporting of which may be important to the RERTR community. Specifically, we will discuss the effect of burnble poison (B_4C) on the irradiation behavior of silicide dispersion fuel, the nature of blister formation during extended postirradiation annealing, and the behavior of a U_3Si fuel plate that operated with breached cladding.

II. Effect of B_4C

Some reactor core designs require the addition of burnable poison in their fuel elements. The most convenient way of incorporating a burnable poison such as ^{10}B is by mixing an appropriate amount of powdered B_4C with the fuel powder. In order to assess the possible effects of such a mixture on the irradiation behavior of silicide dispersion fuel, several U_3Si_2 and U_3Si miniplates containing typical amount of B_4C were fabricated. After irradiation in the ORR to approximately 80% ^{235}U burnup, postirradiation analysis was performed. The results were compared to postirradition data from previously irradiated sibling miniplates that contained no B_4C.

The difference in irradiation behavior between fuel plates with and without B_4C is appreciable. As shown in Table I, the B_4C-containing plates had an average thickness increase of 0.15 mm vs. 0.05 mm for plates without B_4C at approximately the same ^{235}U burnup. Likewise the average meat swelling was 8.6 vs. 2.4%. Metallographic examination reveals the reason for the larger swelling of the B_4C-containing plates. Comparison of polished cross section, (Figs. 1 and 2) clearly show a much larger fraction of retained as-fabricated porosity in the B_4C-containing plates, as well as many clusters of large pores in the fuel particles. The retained as-fabricated porosity was measured with an image analyzer and found to have decreased during irradiation from 10% to 4.5% for the B_4C-containing plates and from 10% to less than 1% for the sibling plates without B_4C (see Table I). Calculating the amount of fuel particle swelling ΔV^F, with the following formula:

$$\Delta V^F = \frac{\Delta V^m + (V_o^P - V^P)}{V_o^F}$$

one obtains, respectively, 31% and 25%. The difference in fuel swelling is presumably due to the presence of pore clusters in the fuel particles of B_4C-containing plates.

In order to further investigate this apparent effect of B_4C on swelling, selected samples were examined with a scanning electron microscope (SEM) including energy dispersive x-ray analysis, and with a scanning Auger electron microprobe (SAM).

Figure 3 shows the distribution of B_4C particles (dark angular features) in an unirradiated fuel plate. The B_4C particles are clearly identified by the boron Auger-electron dot-map shown in Fig. 3.

The meat microstructure after irradiation is also shown in Fig. 3. Again clearly identified by SAM are the B_4C particles, which now appear less angular in shape presumably as a result of irradiation damage. Bigger B_4C particles are found at residual as-fabricated porosity suggesting that the presence of B_4C prevents closure of the pores. Detailed SAM analysis did not detect boron, carbon, or the reaction product lithium in the residual pores. The only other element involved is helium produced through α generation by the reaction:

$$^{10}B\,(n,\alpha)^{7}Li$$

The amount of helium generated in a particle of the size shown in Fig. 3 at complete burnup of the ^{10}B isotope is approximately 7×10^{-10} moles. If all this helium is released into the pore shown in Fig. 1, a pressure of approximately 800 psi could be generated at 100°C. Such a high pressure would certainly prevent closure of the pore, but a lower pressure due to only fractional helium release from the B_4C particle might well be sufficient to prevent pore closure. Without further analyses it seems nevertheless plausible at this point to conclude that helium release is responsible for the observed retention of as-fabricated porosity.

Next we examined the clusters of large pores in the fuel particles that account for the larger fuel particle swelling in the B_4C-containing plates. Optical metallography of etched meat microstructure and a SAM micrograph shown in Fig. 4 reveal a different fuel microstructure around the clusters. The appearance of this etched fuel microstructure is similar to that of fuel that has reacted with aluminum; however, SEM analysis found no difference in composition between the phase around the pores and the bulk of the fuel. SAM analysis again showed no evidence of boron or carbon but a faint indication of lithium was detected.

High magnification SEM examination of the fuel, also shown in Fig. 4 shows the typical small,-regular-spaced fission gas bubbles in the bulk U_3Si_2, but absence of these small bubbles in the different structure around the large pore clusters. Apparently fission gas diffusivity in the cluster area was much higher leading to the growth of large bubbles. We can only speculate that a small amount of lithium and possibly also helium diffused from B_4C particles into adjacent fuel causing a increase to fission gas diffusivity. We believe that there is enough circumstantial evidence to state that activation products from the B_4C particles are the root-cause of the higher swelling of B_4C-containing fuel plates. The effect of B_4C on U_3Si plates was similar to that in U_3Si_2 plates.

III. Blister Formation During Postirradiation Annealing

Blister annealing tests are routinely performed on experimental fuel plates as part of the postirradiation analysis. These tests consist of 1/2 hour annealing steps of 50°C starting at 350°C until blisters are observed. The temperature at which blisters are first formed is called the blister threshold temperature and is a figure of merit to assess the high temperature stability of fuel plates.

To better characterize blister formation long time anneals are performed to study the time-temperature relation of blister formation as well as the behavior of blisters after continued annealing.

The test results are shown in Table II for LEU U_3Si_2 plates with high loading (5.2-5.6 g cm^{-3}) after approximately 85% ^{235}U burnup. The normal blister threshold temperature for this type of plate is 525°C for the standard 1/2 hour anneal. The data in Table II shows that the plates are very stable at 400°C, for no blisters formed after a total time of 696 hours at temperature. The time to form blisters decreases to 327 hours at 425°C and 210 hours at 450°C. No measurable change in plate thickness occurred prior to blister formation at any temperature.

An example of blister formation is shown in Fig. 5. Blisters form typically first at the edges of the fuel core an then at locations throughout the fuel plate. These locations coincide with oxide inclusions at the fuel core-cladding interface (see Fig. 6). Inclusions are usually larger and more numerous at the core edges, hence, the predominant formation of blisters in these areas. During continued annealing blisters, particularly those at the ends of the fuel core grow in size and evenually rupture, as shown in metallographic cross-section in Fig. 7. Fig. 7 also shows the correlation of a large amount of oxide inclusions and large blister formation. Apparently for a blister to continue to grow and rupture, a large amount of oxide needs to be present. This oxide evidently reacts with aluminum and fuel. Fission gas released as a result of this reaction pressurized the blister, eventually rupturing the cladding.

Plates containing B_4C (see previous section) were also subjected to the blister test and were found to have a 100°C lower threshold than plates without B_4C. The blisters in these plates were also more numerous after prolonged annealing (see Fig. 8). A cross-section though some blisters, also shown in Fig. 8, reveals that the blisters form at the fuel core-cladding interface. Oxide inclusions are the most likely initiation sites; however, it seems plausible that helium originating from the n-α reaction in the B_4C particles diffused to these sites and pressurized the blisters, thereby promoting their growth.

IV. Operation with Breached Cladding

Coolant channel width between miniplates is routinely measured during scheduled shutdowns in the ORR irradiation program. During one of these measurements a significant decrease in channel width was observed in two adjacent channels in irradiation module 34. The change was not large enough to require removal of the module and the irradiation was continued. After an additional reactor run, the same channels were found to have changed drastically and the module was removed for examination. Photography of the module using backlighting through the coolant channels showed one severely pillowed plate, see Fig. 9. The plate in question was an LEU U_3Si plate with a loading of 6.1 g cm^{-3} that had accummulated a ^{235}U burnup of 55%. Visual examination of this plate after removal from the module revealed a transverse crack at one end of the pillow near the end of the fuel core. Also, the channel width probe had gouged the cladding on the pillow, as shown in Fig. 9.

A metallographic section was taken at the end of the pillow transecting the crack as shown in Fig. 10. The crack is located at the "dog bone" end of the fuel core where the cladding is rather thin. There is a large amount of two phase reaction product in the area and this reaction product contains large fission gas bubbles. The cladding breached probably early on during the irradiation in a very thin spot over the dog bone end. Ingress of water during continued irradiation resulted in the reaction (most likely oxidation) of the silicide - Al dispersion. Fission gas bubbles evidently grow easily in the reaction product, although hydrogen originating from the decomposition of H_2O may also have contributed to bubble growth. The reaction product, including its gas bubbles, appears similar to the fuel core phases found in high burnup - highly loaded U_3O_8-Al fuel plates where the U_3O_8 has completely reacted with the aluminum matrix.[1] It is of interest to note that predefected fuel plates when soaked in hot water for prolonged periods [2] do not show the formation of interaction product and do not swell; evidenty radiation is necessary for the reaction to occur. No unusual fission gas activity was detected during the irradation and release of fission gas through the crack, which must have occurred to some extent, was evidently of such a low rate that the ORR instrumentation could not measure it.

German investigators have reported on operation with a failed U_3Si_2 miniplate [3]. The cladding of this plate had cracked at a thermocouple attachment point and also had also developed a pillow at the crack site.

It is interesting to note that experimental UAl_x-Al dispersion miniplates irradiated in the Advanced Fast Reactor, ATR, with cladding corrosion defects also developed pillows [4].

References

1. G. L. Hofman et al., Nucl. Technol. Vol. 72, Mar. 1986, pp. 330-344.
2. R. F. Domagala, Argonne National Laboratory, Private Communication.
3. C. Thamm, KFA, Jülich personal communication, and W. Krug etc., this meeting.
4. J. M. Beeston et al., Idaho National Engineering Laboratory, EGG-SE-6696, Oct. 1984.

TABLE I. Comparison of LEU, U_3Si_2 Miniplates With and Without B_4C

	With B_4C	Without B_4C
^{235}U Loading, g cm^{-3}	5.1	5.1
Δt, in. (mm)	0.005 (0.15)	0.0021 (0.05)
ΔV^m, %	8.6	2.4
ΔV^F, %	31	25
V_o^F, %	46	46
V_o^P, %	10	10
V^P, %	4.5	1.0
FD^m, 10^{21}	1.9	2.2
Bu, %	79	84
Blister Temp, °C	425	525

where:

Δt is plate thickness increase, including oxide layer.

ΔV^m is meat volume change $\dfrac{V^m - V_o^m}{V_o^m}$

ΔV^F is fuel particle volume change.

V_o^F is the original fuel volume fraction in meat.

V_o^P is the original as-fabricated porosity in meat.

V^P is the fraction of as-fabricated porosity remaining after irradiation.

FD is the accumulated fission density.

TABLE II. Postirradition Annealing Data of U_3Si_2 Miniplates

Plate A-99, 5.2 g cm^{-3}, 79% Bu, 400°C

time, hours	Thickness, mils: Grid Point* 5	6	7	Comments
0	62.0	61.5	61.4	
6	62.0	61.5	61.4	
47	62.0	61.3	61.3	
117	62.0	61.3	61.3	
313	62.5	61.3	61.3	
531	61.8	61.3	61.3	
696	--	61.2	61.4	No Blisters

Plate A-91, 5.6 g cm^{-3}, 84% Bu, 425°C

time, hours	5	6	7	Comments
0				
257	50.0	50.3	50.2	
327	50.6	50.2	50.0	One Blister
423	50.0	61.0	50.2	3 Blisters Warping
517	58.0	61.0	50.2	7 Blisters Warping

Plate A-85, 5.0 g cm^{-3}, 84% Bu, 450°C

time, hours	5	6	7	Comments
0	51.0	51.0	51.4	
20	51.0	51.0	51.4	
115	51.8	51.2	51.5	
210	53.0	53.1	53.0	Blister in Center
278	54.1	55.0	54.8	U + Warping
490	73.0	68.0	60.7	Many Small Blisters and Warping

*These points are spaced on the longitudinal center line of the plates.

Fig. 1. Microstructure of Plate A-199P, U_3Si_2 & B_4C, Showing Retained As-Fabricated Porosity and Bubble Clusters in Fuel After Irradiation

Fig. 2. Microstructure of Plate A, U_3Si_2 Without B_4C, Showing Nearly Complete Closure of As-Fabricated Porosity and Absence of Bubble Clusters

(210716) SAM, Specimen Current

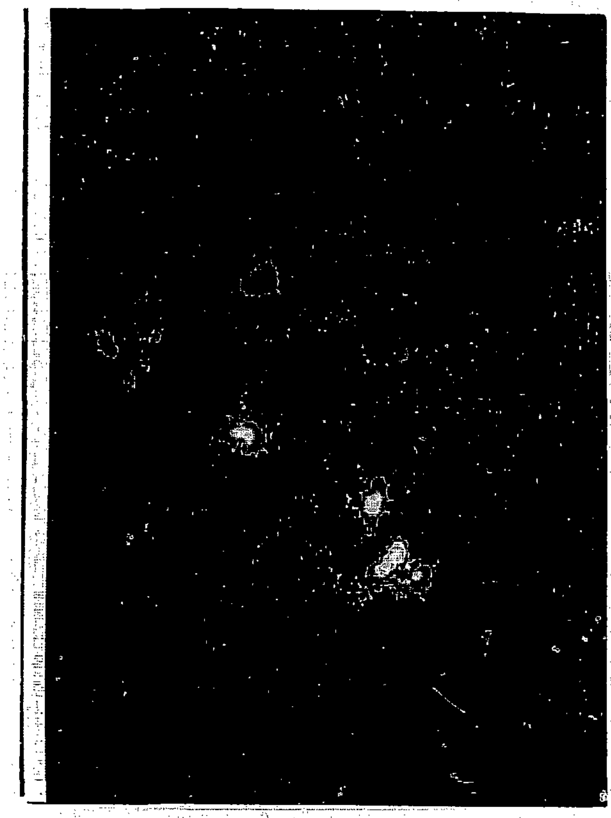

(210717) SAM, Boron

SEM

(210739) SAM, Boron, Detail

Fig. 3. Fuel Core Microstructure Showing B_4C Particles,
Upper: Unirradiated; Lower: Irradiated

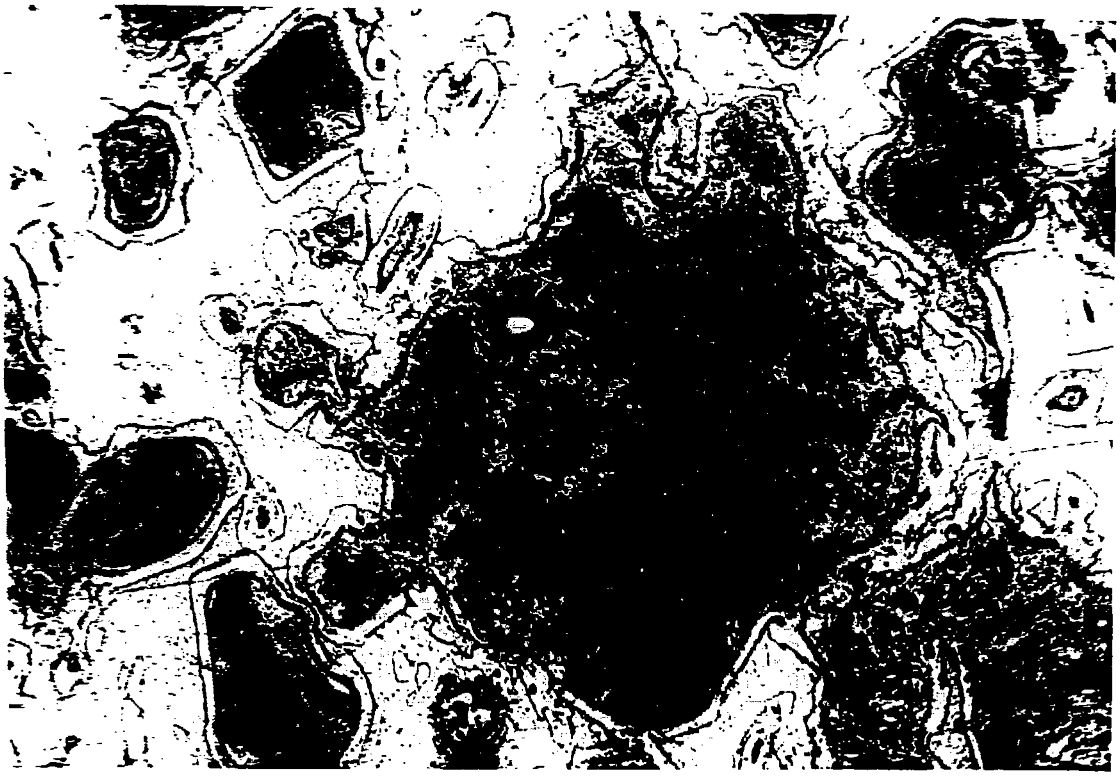

Optical Etched

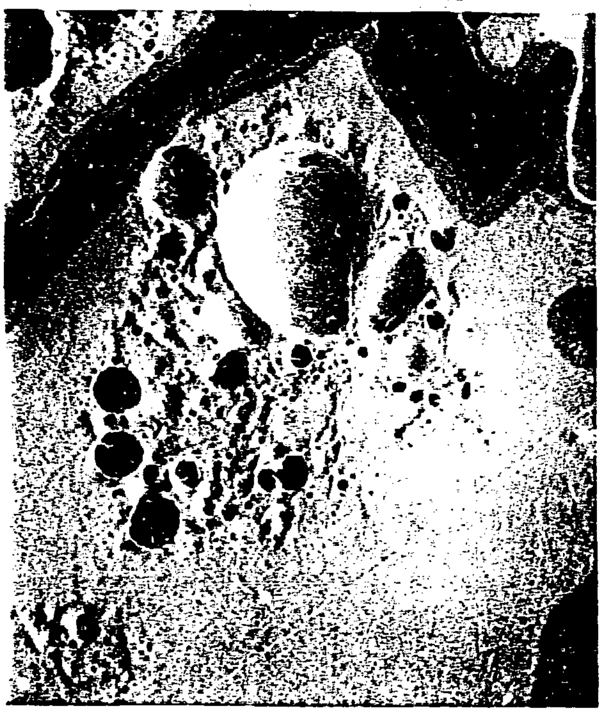

SAM

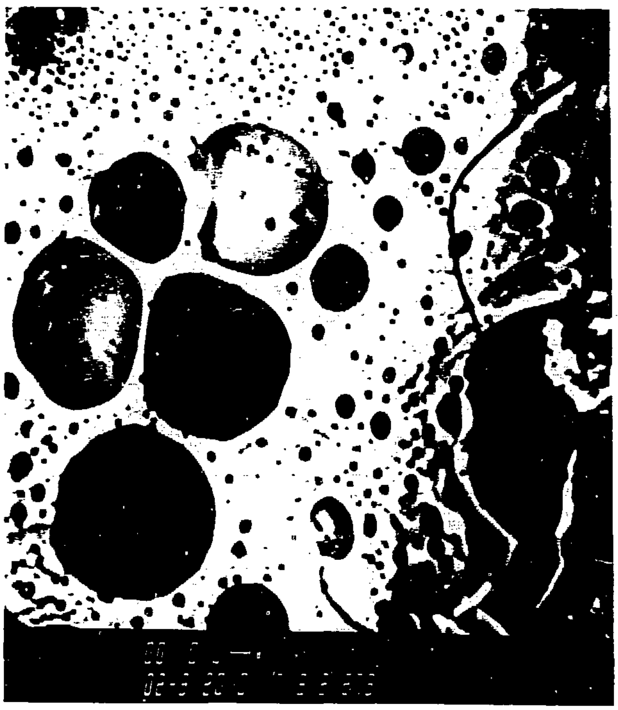

SEM

Fig. 4. Fuel Microstructure Showing Structural Difference Around Bubble Clusters in Fuel Particles

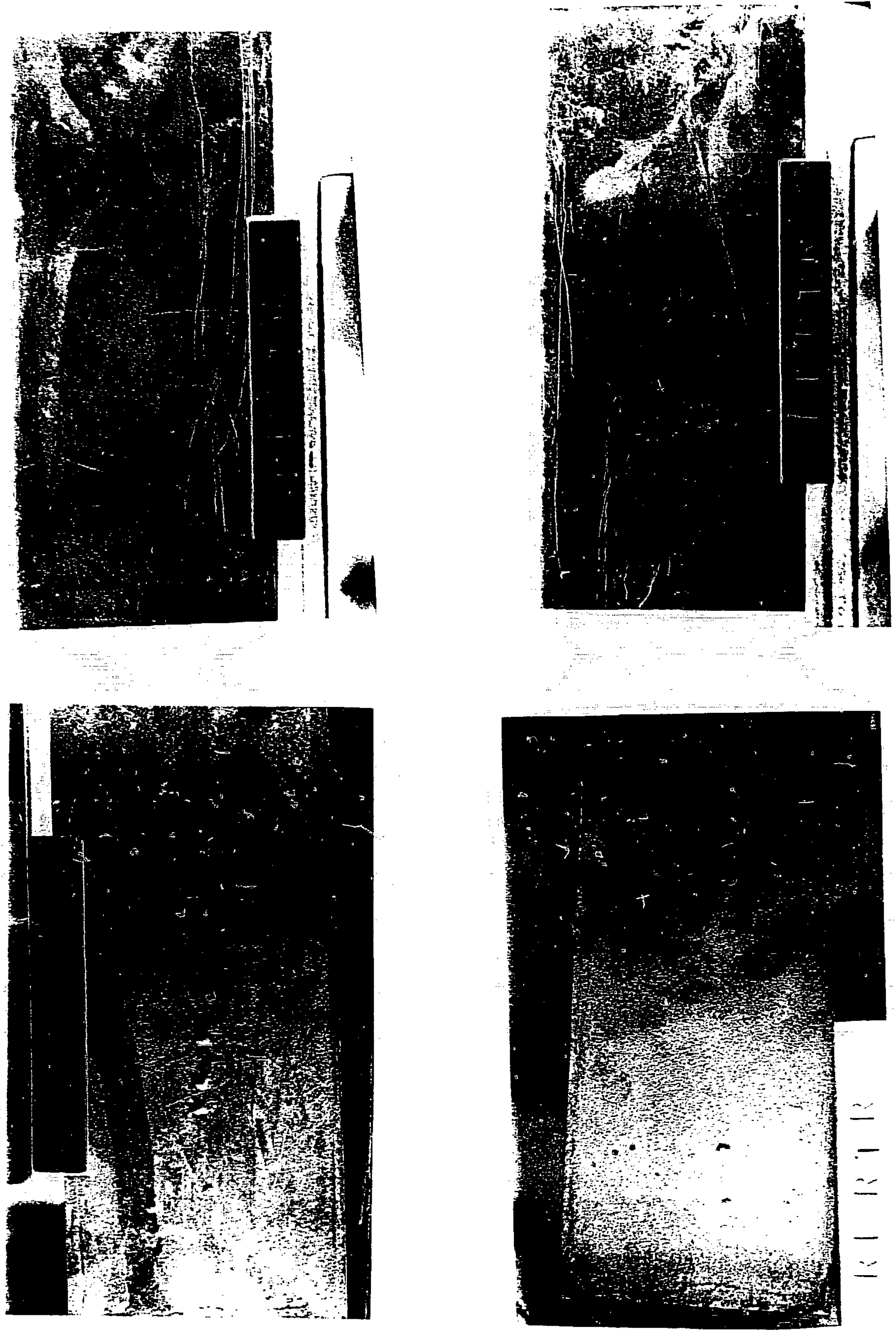

Fig. 5. Location of Blisters in Irradiated U_3Si_2 Plates After 1/2 Hour at 525°C

Fig. 6. Fuel Core Microstructure of Irradiated U_3Si Plate Showing Location of Oxide Particles at Core Edge and Dog Bone End

Fig. 7. Crossection of Ruptured Blister at Dog Bone End of Irradiated U_3Si_2 Plate After Prolonged Annealing at 450°C

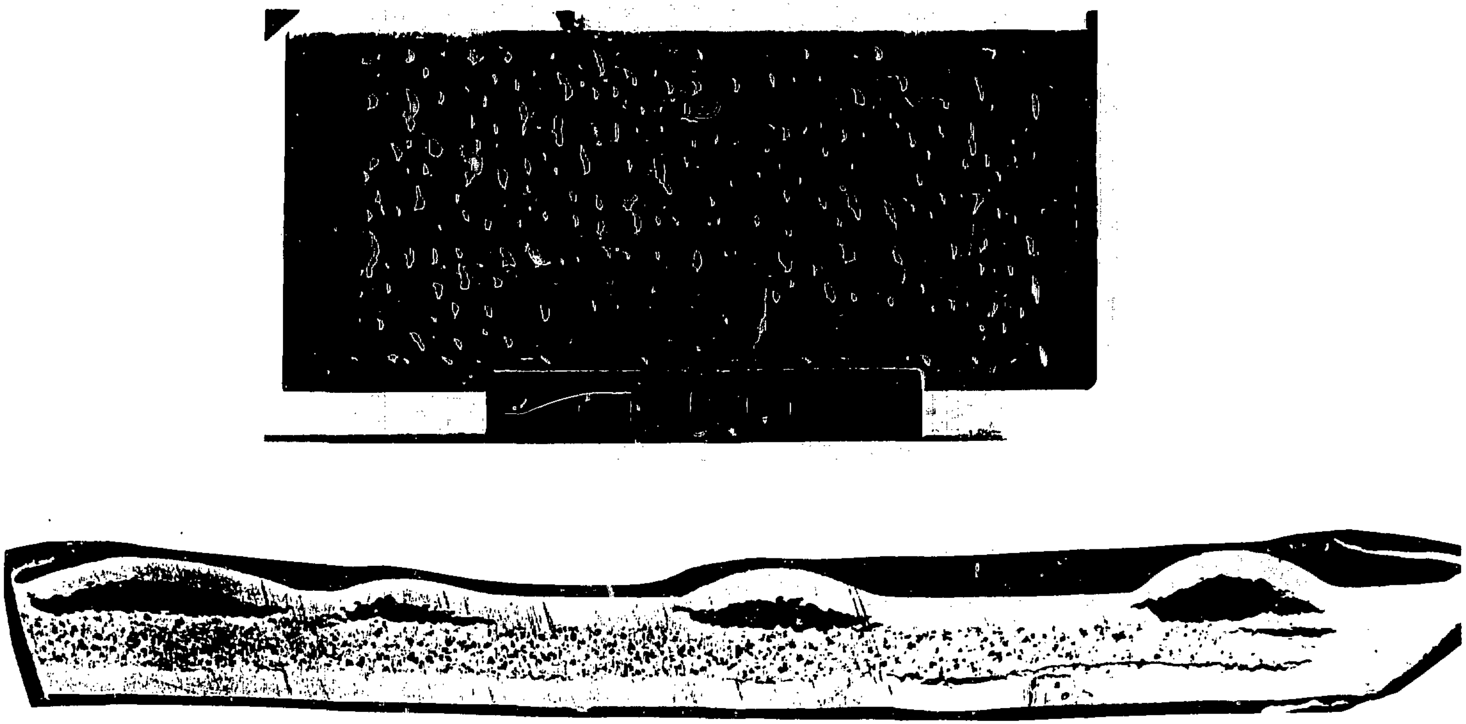

Fig. 8. Blisters and Crossection Through Blisters of B_4C Containing U_3Si_2 Plate after Prolonged Annealing at 450°C

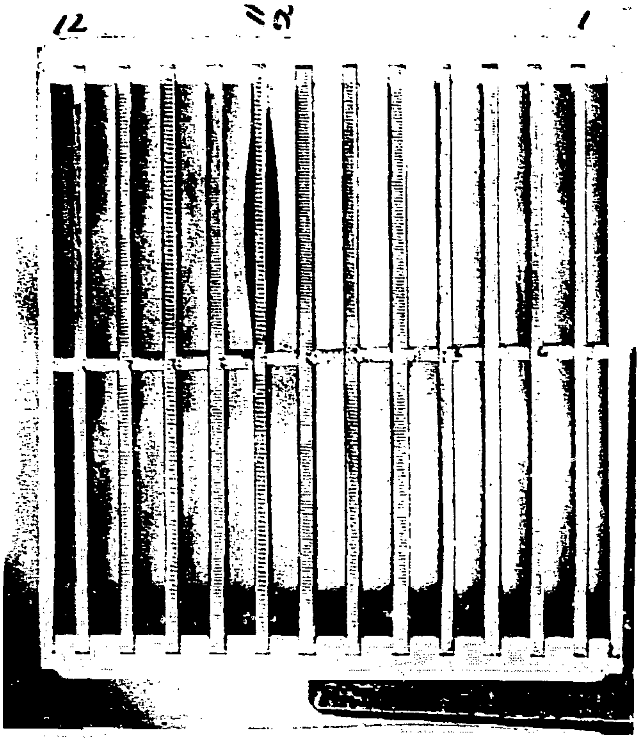

Back lightening through module

Edge on view of pillowed plate

Fig. 9. Views of Pillowed U_3Si Plate A211, Showing Crack of Edge of Pillow

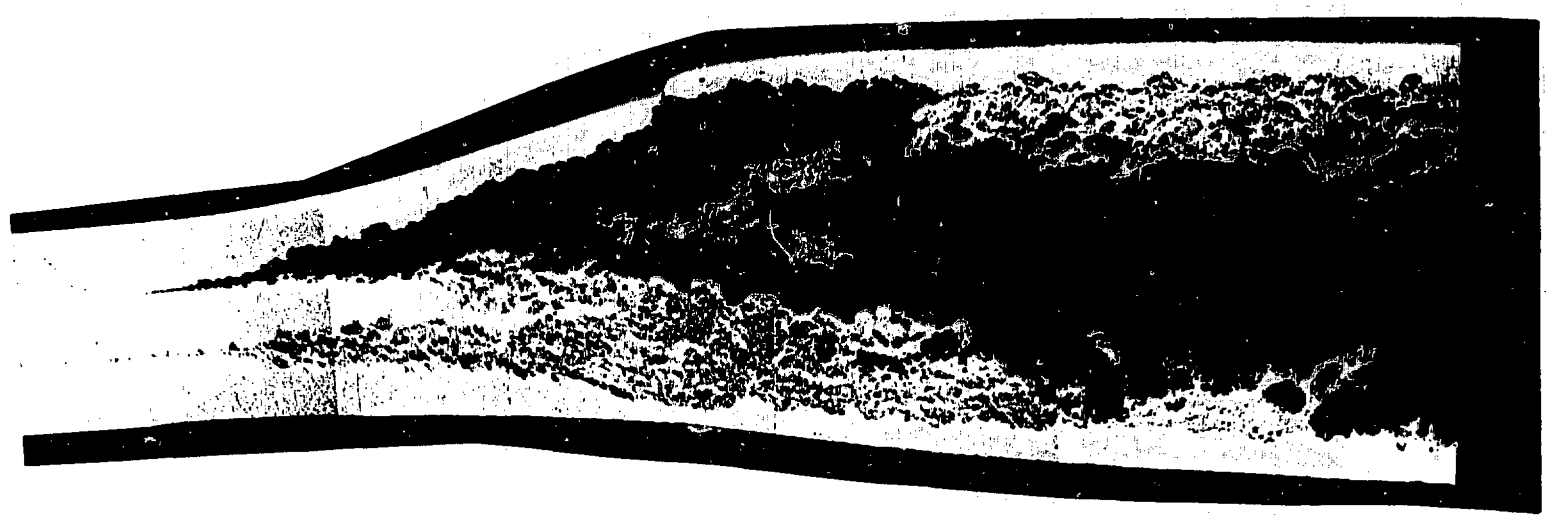

Detail

Fig. 10. Crossection of Pillowed Region of Plate 211, Including Crack Showing Remnants Reaction Product